ADVANCED MATERIALS
www.advmat.de

Insights into the Si—H Bonding Configuration at the Amorphous/Crystalline Silicon Interface of Silicon Heterojunction Solar Cells by Raman and FTIR Spectroscopy

Benedikt Fischer, Andreas Lambertz, Maurice Nuys, Wolfhard Beyer, Weiyuan Duan, Karsten Bittkau, Kaining Ding, and Uwe Rau*

In silicon heterojunction solar cell technology, thin layers of hydrogenated amorphous silicon (a-Si:H) are applied as passivating contacts to the crystalline silicon (c-Si) wafer. Thus, the properties of the a-Si:H is crucial for the performance of the solar cells. One important property of a-Si:H is its microstructure which can be characterized by the microstructure parameter *R* based on Si—H bond stretching vibrations. A common method to determine *R* is Fourier transform infrared (FTIR) absorption measurement which, however, is difficult to perform on solar cells for various reasons like the use of textured Si wafers and the presence of conducting oxide contact layers. Here, it is demonstrated that Raman spectroscopy is suitable to determine the microstructure of bulk a-Si:H layers of 10 nm or less on textured c-Si underneath indium tin oxide as conducting oxide. A detailed comparison of FTIR and Raman spectra is performed and significant differences in the microstructure parameter are obtained by both methods with decreasing a-Si:H film thickness.

1. Introduction

In light of the current political, ecological, and environmental dynamics, there is a pressing need to expand the production of solar cells. Such an expansion demands a technology that is not only suitable for large-scale industrial implementation but also excels in terms of solar cell efficiency. The Silicon Heterojunction (SHJ) solar cell technology stands out as a prime candidate, boasting a remarkable combination of minimal processing steps and an impressive track record of efficiency. Notably, it has achieved a published efficiency record of 26.81% for silicon-based solar cells.[1] To mass produce solar cells with efficiencies in this range, a precise understanding of the interdependence between deposition conditions, the properties of the layers, and the solar cell performance is required.[2] Most concepts of highly efficient SHJ solar cells use intrinsic hydrogenated amorphous silicon (a-Si:H) films, which are also used in other devices such as diodes, thin film transistors, or batteries.[2–5] In SHJ solar cells, aSi:H films with very low thicknesses act as passivating contact layers to the crystalline silicon (c-Si) wafer.[6–8] In the future, silicon wafers will become thinner requiring higher passivation quality compared to current solar cells, because interface recombination will be more limiting compared to bulk recombination. Therefore, the microstructure of the a-Si-H layer and especially the microstructure close to the interface is highly important for the performance of the solar cell.[1,9–12] The Si—H bond configuration provides information about the microstructure (i.e., giving information if the a-Si:H has a dense or void-rich structure).[13,14] Hydrogen plays a decisive role since free bonds are saturated and defective ones are passivated. Thus, the Si—H bond configuration is of great interest and is usually analyzed by Fourier transform infrared (FTIR) spectroscopy on thicker films than used for SHJ solar cells.[9,10,15,16] In FTIR spectra, absorption peaks of Si–H wagging modes occur at 640 cm^{-1}, Si—H bending modes at 840 to 890 cm^{-1} and Si—H stretching modes at 2000 to 2100 cm^{-1}.[17] While any H in a-Si:H is assumed to contribute to the wagging and stretching modes, bending modes are only visible for Si—H_2 (and maybe Si—H_3) bonding configurations.[13,14,17–19] Due to the amorphous structure of a-Si:H, in principle all these modes are also Raman active.[18] Nevertheless, the relative signal strength of two vibrational modes within one spectrum can vary between both methods, FTIR and Raman spectroscopy, due to the different detection principles via photon absorption and Raman

B. Fischer, A. Lambertz, M. Nuys, W. Beyer†, W. Duan, K. Bittkau, K. Ding, U. Rau
IEK-5 Photovoltaik
Forschungszentrum Jülich GmbH
Wilhelm-Johnen Straße, 52425 Jülich, Germany
E-mail: b.fischer@fz-juelich.de
B. Fischer, U. Rau
Jülich Aachen Research Alliance (JARA-Energy) and Faculty of Electrical Engineering and Information Technology
RWTH Aachen University
Schinkelstr. 2, 52062 Aachen, Germany

The ORCID identification number(s) for the author(s) of this article can be found under https://doi.org/10.1002/adma.202306351

†Wolfhard Beyer passed away in the course of the publication process.

DOI: 10.1002/adma.202306351

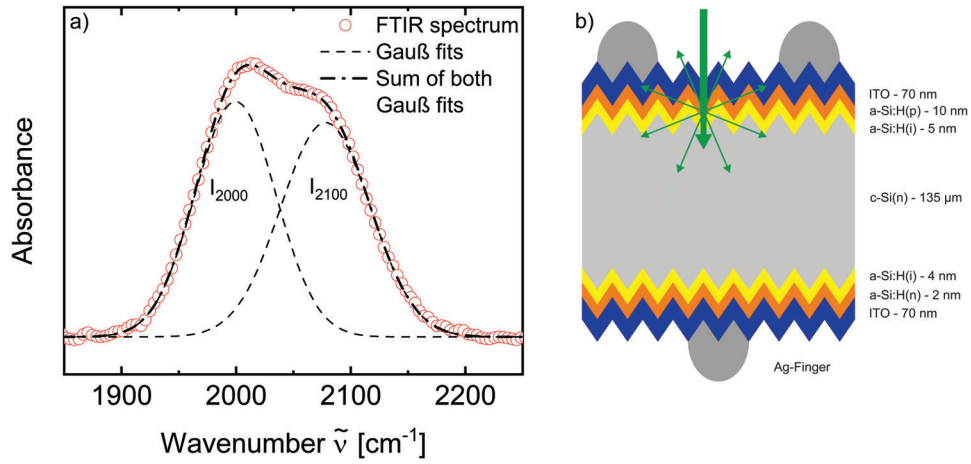

Figure 1. a) A typical spectrum of the vibrational modes of Si—H bonds in a-Si:H measured by FTIR spectroscopy. The corresponding Raman spectrum is similar. b) Schematic of the Raman laser beam entering the SHJ solar cell and Raman scattering at the a-Si:H layers.

scattering, respectively.[18] Here we focus on the Si—H stretching modes, of which a typical FTIR spectrum for aSi:H in the 2050 cm^{-1} range is shown in **Figure 1**a). The spectrum can be decomposed into two Gaussian peaks centered at wavenumbers of ≈2000 and 2100 cm^{-1}. In dense material, only the peak at 2000 cm^{-1} is observed whereas in void-rich/porous material Si—H bonds occur more at internal surfaces which manifests in the peak at 2100 cm^{-1}.[17,20] It is worth noting that the peak centers are only representatively called 2000 and 2100 cm^{-1}. Due to varying electrical screening occurring from differences in the dielectric film properties surrounding the Si—H bonds, the peak centers can be shifted.[21] Therefore, besides the peak area and width also the peak center was defined as a fit-parameter of the least-square fit. We found Gaussian peaks centered in the range from 1990 to 2020 cm^{-1} and from 2070 to 2100 cm^{-1} respectively. The robustness of the fits was demonstrated by varying the initial parameters. The ratio of the 2100 cm^{-1} integrated absorption I_{2100} to the integrated absorption of both peaks is called the microstructure parameter $R = I_{2100}/(I_{2100} + I_{2000})$.[22,23] Using the FTIR absorption coefficient α and the wavenumber ω, the integrated absorption is $I = \int \omega^{-1}\alpha(\omega)\, d\omega$.[14,17] It has been reported that the microstructure parameter of very thin a-Si:H films can be significantly higher compared to thicker a-Si:H.[24,25] This has been attributed to nucleation effects. In addition, recently, Zhao et al.[26] reported significant changes of the spectra-shape in the 640 cm^{-1} range with varying film thicknesses (14–162 nm). To get further insights into these effects, we investigate a-Si:H films (2–60 nm) not only with FTIR but also with Raman spectroscopy, analyze the difference in the spectra of both characterization techniques, and use it as a tool. By comparing the spectra of FTIR and Raman spectroscopy and calculating the microstructure parameter R for both methods, we investigate the microstructure of nucleation layers in more detail.[16] For the calculation of R from Raman spectra we used the peak intensities I_{2000} and I_{2100} defined as the areas below two Gaussian functions fitted to the Raman intensity.[27] The thickness of a-Si:H nucleation layers is at the same scale as the total thickness ($d \approx 2$–3 nm) of the intrinsic a-Si:H layers (i1-layers) used in SHJ solar cells to passivate the c-Si surface.[16,28] Additionally, subsequent processes like annealing or post-hydrogenation (e.g., in a hydrogen plasma) can change the microstructure of the a-Si:H films.[29–31] Therefore, it is of great interest to measure the microstructure parameter of the a-Si:H thin films directly on a finished device like a SHJ solar cell. Scattering of the IR-light on textured surfaces of c-Si wafers, free carrier absorption in transparent conducting oxide (TCO) contact layers (like indium tin oxide (ITO)), and the fact that aSi:H layers may be on both sides of an (SHJ) solar cell make FTIR spectroscopy measurements in transmission mode and its evaluation difficult. In this work, we use the method of Raman spectroscopy using a laser with a wavelength of 532 nm so that the light can pass the ITO-layer but not the c-Si wafer, making an independent investigation of the a-Si:H layer on both sides, the p-side and the n-side possible, as depicted in Figure 1b).[32,33] The concept is tested on samples with various a-Si:H layer thicknesses and microstructures. A detailed comparison of FTIR and Raman spectroscopy is performed to properly evaluate and classify Raman spectroscopy spectra measured on a-Si:H films on solar cells.

2. Results

In the baseline SHJ solar cells investigated at Jülich, the thicknesses of the (i/n, i/p) a-Si:H layer stacks are ≈6 nm on the n-side and 15 nm on the p-side.[34] Raman and FTIR spectra were measured on layers on HF-etched c-Si wafers prepared by using the same recipes as used for the underdense i1 layer and the more dense i2 layer in solar cells.[2,28,34,35] The deposition power of the underdense layers was set to 100, 200, 300, and 400 W to vary the microstructure of the layers and so the Si—H stretching mode signals in Raman and FTIR spectra. In this series of films, the deposition time and the film thickness were varied too. **Figure 2**a,b shows the corresponding spectra of the layers deposited at $P_p = 300$ W at different thicknesses. The Raman measurements were scaled with the corresponding film thickness and a constant factor for all films for better visual comparability with the FTIR measurements. In comparison with the Raman spectra, FTIR spectra show a more pronounced peak at 2100 cm^{-1} for all thicknesses. FTIR spectra reveal a strong

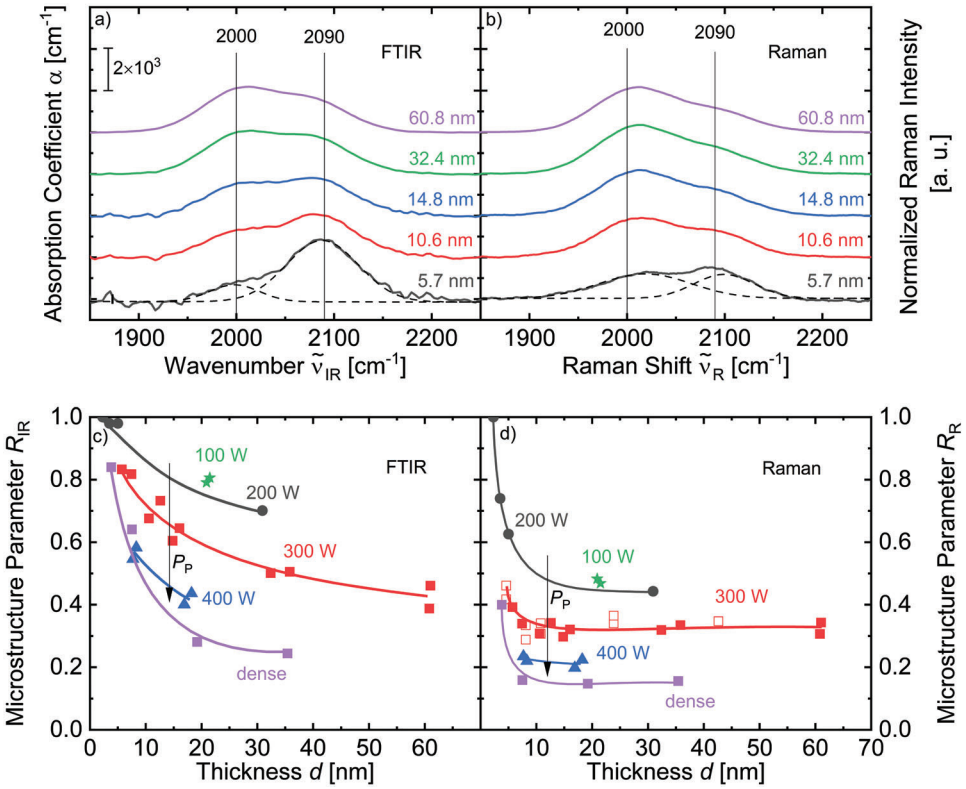

Figure 2. a) FTIR absorption spectra and b) corresponding Raman intensity spectra normalized by the layer thickness of intrinsic a-Si:H layers of various thicknesses deposited at $P_P = 300$ W versus the wavenumber $\tilde{\nu}_{IR}$ and the Raman shift $\tilde{\nu}_R$, respectively. The sample thicknesses are indicated on the right side of the graphs. The dashed lines show the double Gaussian function fits for the film of 5.7 nm thickness. Layer thickness dependency of R determined by c) FTIR and d) Raman spectroscopy spectra of intrinsic a-Si:H layers with thicknesses of 2.3–60.8 nm of four i1-layers (with indicated plasma powers) and an i2-layer (dense). For the deposition at 300 W, in addition to films on polished wafers (filled squares), films on textured wafers (hollow squares) are measured using Raman spectroscopy. The lines are guides to the eye.

thickness dependency of the overall contribution of the 2100 cm^{-1} peak. The thinner the film, the larger the contribution from the 2100 cm^{-1} peak. In agreement with that, a similar pronounced peak at 2100 cm^{-1} for thinner films was also found by infrared attenuated total reflection spectroscopy measurements from Fujiwara et al.[24] but in that case, the substrate was not HF etched c-Si (as the substrate of the samples in Figure 2) but c-Si with 30 Å native SiO_2. Nevertheless, our results are comparable to the measurements of Fujiwara et al.,[24] as we found for our underdense films that the initial growth process is similar for Hf-etched substrates and substrates with native SiO_2.[16] In contrast to FTIR, the Raman spectrum between 1900 and 2200 cm^{-1} turns out to be nearly thickness-independent, except for a slightly more pronounced peak at 2100 cm^{-1} for the 5.7 nm film. These trends are clearly visible in Figure 2c,d that show microstructure parameters R_{IR} and R_R of the spectra in Figure 2a,b and other spectra of films deposited with different plasma powers and deposition times. The microstructure parameters were determined by fitting the FTIR and Raman spectra with Gaussians and are plotted as a function of the layer thickness in Figure 2c determined with FTIR spectra (R_{IR}) and d) determined with Raman spectra (R_R).[17] From Maurer et al.,[27] based on work by Volodin and Koshelev,[36] it is known that spectra measured by both methods for thick layers (>500 nm) result in a similar R. However, for the thin samples used in this work, R determined from FTIR spectra is higher than R determined from Raman spectra for all deposition powers and thicknesses. Additionally, R determined from the FTIR spectra decreases asymptotic with increasing layer thickness, in contrast to R determined by Raman spectra, which is almost constant for a-Si:H layers with $d > 10$ nm. For very thin layers lower than 10 nm R measured by Raman increases with decreasing layer thickness. This increase can be seen especially for the 200 W i1-layer and the i2-layer because of low film thicknesses down to 2.3 and 3.8 nm, respectively. For thicker layers, the R measured using FTIR spectroscopy approaches the R measured using Raman spectroscopy as can be seen for the 300 W deposition series, which is measured over a wide thickness range up to 60 nm. R measured on textured samples (hollow squares) follows a similar trend as measured on polished samples (filled squares). For both FTIR and Raman spectroscopy, the microstructure parameter decreases with increasing deposition power and the microstructure parameter of the i2-layer is the lowest. Raman spectroscopy measurements by Macco et al.[37] showed similar Si—H stretching signals for various samples of 10 nm thickness deposited at temperatures of 10 to 50 °C. Despite the low temperature and sample thickness, they also found a relatively low microstructure parameter of 0.3–0.4 in agreement with our results for the underdense material. With regard to results obtained by FTIR spectroscopy, data on a-Si:H films of thicknesses

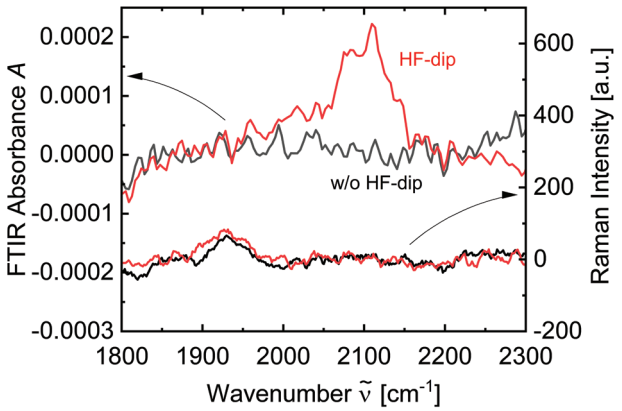

Figure 3. FTIR spectra and Raman spectra with an adjusted scale of two polished p-type wafers with HF-dip directly before the measurement (red) and without HF-dip (black).

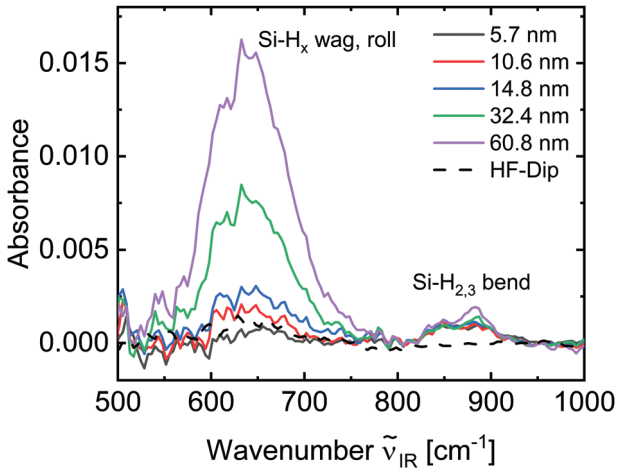

Figure 4. Layer thickness dependency of R determined by FTIR spectroscopy spectra [squares] of intrinsic a-Si:H layers and calculated R using the model explained in the text [dashed lines].

near 10 nm have been published by various authors.[38–40] For example, by Wu et al.[38] an FTIR microstructure parameter $R = 0.65$ was reported for hot wire grown underdense a-Si:H while for dense material a microstructure parameter of 0.25 was reported. Thus, our results in Figure 2c ($R \approx 0.7$ for 10 nm thickness and $P_p = 300$ W) are consistent with their underdense a-Si:H. A high microstructure parameter can also be observed for the underdense a-Si:H used by Liu et al.[28] for obtaining highly efficient SHJ solar cells. Although the results of the Raman and FTIR spectra each fit to corresponding literature, the reason for the difference between both methods is still unclear but can be of great relevance for the passivation and the resulting solar cell performance. Therefore, we investigated the a-Si:H/c-Si interface and the Si—H bonds located there in more detail as a first approach to find the reasons for the difference in the spectra of both methods.

Figure 3 shows spectra of a p-type c-Si substrate measured by FTIR and Raman directly after the HF-dip (red curves) and without HF dip (black curves) for comparison. The y-axis of the Raman spectra is scaled in the same way as in Figure 2b. The FTIR spectrum of the sample with HF-dip shows a peak at 2100 cm^{-1} which is not present without HF dip. No peak near 2100 cm^{-1} is visible in the Raman spectra for both with and without HF dip. As the FTIR peak at 2100 cm^{-1} can be attributed to hydrogen bound to the c-Si surface,[13,41–43] the results demonstrate that our Raman setup is not sensitive to hydrogen at the c-Si surface, which is in agreement with observations by Spizziri et al.[44] Thus, the difference between Figure 2c,d can partly be explained by the lacking contribution of hydrogen on the c-Si surface to the Raman 2100 cm^{-1} signal. However, the integrated FTIR absorbance in Figure 3 of surface hydrogen is too low, to fully explain the difference between R_{IR} and R_R.

In order to clarify the impact of c-Si surface Si—H bonds on the overall FTIR spectrum, we calculated the FTIR microstructure parameter by a model that relies on an H-rich interface to the c-Si where all the Si—H bonds contribute to the 2100 cm^{-1} peak in the FTIR spectrum. Within this model, the Si–H peak intensity has three contributions. The intensities i) I_{2000} and ii) I_{2100} from the Si—H bonds in the homogeneous a-Si:H layer and the intensity I_{int} which occurs from Si—H bonds at the interface contributing to the 2100 cm^{-1} peak. Therefore, within this model the calculated microstructure parameter R_c is $R_c = (I_{2100} + I_{int}) / (I_{2100} + I_{2000} + I_{int})$.

By definition, I correspond to a volume density of bonds. By multiplying an absorption strength constant A with I, an average for the number density n of H atoms can be calculated by $n = A \times I$. Inserting a plane with an area density of n' into a film with a volume density of $n = 0$ and a thickness of d leads to an average number density of $n = n'/d$.

Therefore, assuming a surface hydrogen absorption strength constant A_{int}, the intensity I_{int} of Si—H bonds at the interface can be estimated by

$$I_{int} = \frac{n_{int}(H)}{A_{int}} = \frac{n'_{int}(H)}{d\,A_{int}} \quad (1)$$

Dividing the area number density n'_{int}(H) by the film thickness d gives the H volume density n_{int}(H), to which the Si—H interfacial bonds in the a-Si:H bulk would contribute. For an absorption strength constant $A = A_{2000} = A_{2100}$,[17] the microstructure parameter R_c expected for FTIR spectroscopy can be calculated knowing the microstructure parameter R_{a-Si} of the a-Si:H bulk layer and the hydrogen density n_{a-Si}(H) in the bulk layer by

$$R_c = \frac{R_{a-Si}\frac{n_{a-Si}(H)}{A} + \frac{n'_{int}(H)}{d\,A_{int}}}{\frac{n_{a-Si}(H)}{A} + \frac{n'_{int}(H)}{d\,A_{int}}} = \frac{R_{a-Si}\,n_{a-Si}(H) + \frac{n'_{int}(H)}{d\,\beta}}{n_{a-Si}(H) + \frac{n'_{int}(H)}{d\,\beta}} \quad (2)$$

where β is the ratio of the absorption strengths constant A_{int} to A. From FTIR, we determined the hydrogen contents c(H) to 20–30% for the films from Figure 2 using an absorption strength constant of $A = 1 \times 10^{20}$ cm^{-2}.[17] The hydrogen density can then be calculated by n(H) = c(H) × n(Si).

Figure 4 shows the measured and calculated thickness dependencies of R determined using FTIR spectra. For R_{a-Si} we used the value observed by Raman spectroscopy of the films with $d > 10$ nm. Using β as a fit parameter, we aligned our calculated curves to the measurements as shown in Figure 4.

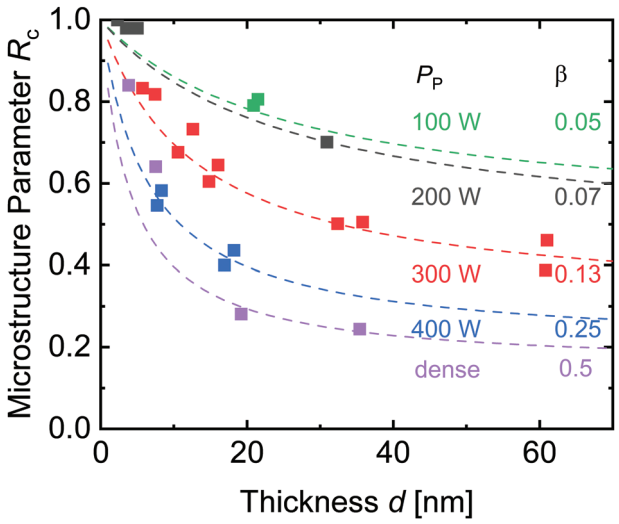

Figure 5. FTIR absorbance spectra of the intrinsic a-Si:H layers from 2 a) and a wafer only with HF-dip (Figure 3) versus the wavenumber $\tilde{\nu}_{IR}$. The Si–H vibrational modes corresponding to the peaks in the spectrum are labeled within the graph.

For $n'_{\mathrm{int}}(\mathrm{H})$ we assumed 1 monolayer of hydrogen, that is, $n'_{\mathrm{int}}(\mathrm{H}) = n'_{\mathrm{int}}(\mathrm{Si}) = (n_{\mathrm{Si}}(\mathrm{Si}))^{2/3} = 1.35 \times 10^{15}$ cm^{-2}. With decreasing deposition power, the ratio β of the absorption strength constants also decreases. For a plasma power of 100 W, the calculated R fits well for $\beta = 0.05$, that is, the absorption strength constant for the Si—H bonds in the bulk a-Si:H is twenty times higher than at the interface. The absorption strength constant on c-Si might be lower than in the bulk, for example, due to the variation in the dielectric properties of the material.[14,18,45] However, a 20-fold increase in the absorption strength constant may not be realistically feasible. On the other hand, assuming an $A_{int} \approx A$, the fitted ratio β can represent different amounts of Si—H bonds, maybe not only at the c-Si surface but also in the island-like grown nucleation region of the a-Si:H layer.[24,46] For the film deposited at 100 W this would correspond to a H content of 50% within the first 10 nm of the layer, which is close to the maximum theoretical limit.[47] Films with such high H content can have a polysilane-like structure.[18] Therefore, within the nucleation region, the amount of Si—H_2 and Si—H_3 bindings can be increased and mostly contribute to the 2100 cm^{-1} peak.[14,18,24] Fujiwara et al.[24] observed a shift of the 2100 cm^{-1} peak within the nucleation layer caused by Si—$H_{2/3}$ modes, which was also observed for our films <5 nm by both methods, FTIR and Raman spectroscopy. In addition to the stretching modes, bending modes at the wavenumber range from 840 to 890 cm^{-1} are observed for Si—$H_{2,3}$ bonds.[13,14] **Figure 5** shows FTIR absorption spectra of the Si—$H_{2,3}$ bending modes (840–890 cm^{-1}) and wagging and rolling modes (640 cm^{-1}) which are observed for any H bonded to Si.[17] The spectra are of the same films investigated in Figure 2a. The peak at 640 cm^{-1} increases with increasing film thickness due to the higher amount of Si—H bonds. In contrast, the peaks at 840 and 890 cm^{-1} remain constant. Additionally, the bending peaks are not visible for the spectra of the H-covered wafer (HF-Dip). Thus, the nucleation layer of our films indeed incorporates a high amount of Si—$H_{2,3}$ bonds leading (besides H on the c-Si surface) to an increased 2100 cm^{-1} peak and therefore an increase of the R_{IR} with decreasing film thickness.

The Si—$H_{2,3}$ stretching modes contributing to the 2100 cm^{-1} peak can have different Raman activities in comparison with the Si—H stretching modes maybe contributing to the difference between R_{IR} and R_R.[14,18] This result fits also to our assumption of an increased H amount contributing to the 2100 cm^{-1} peak near the interface for the R_c calculation in Figure 4. The possibly decreased Raman activity of Si—$H_{2,3}$ modes is interesting for future investigations and opens more insight into the Si—H bonding structure near the interface.[14]

Knowing the limitations of the Si—H Bond detection and the difference to FTIR spectroscopy, we use Raman spectroscopy to investigate the R of the a-Si:H layers in solar cells. Therefore, we studied the influence of an ITO layer on top of intrinsic a-Si:H layers for various microstructures caused by varying the plasma-enhanced chemical vapor deposition (PECVD) plasma power P_P from 100 to 400 W. **Figure 6**a shows the Raman spectra normalized to its maximum. The Si–H spectra after ITO deposition have the same shape as the spectra before ITO deposition except for a slight difference between the two spectra of the layer deposited at $P_P = 100$ W. Figure 6b shows the microstructure parameter $R_{\mathrm{w\,ITO}}$ measured after ITO deposition dependent on the microstructure parameter $R_{\mathrm{w/o\,ITO}}$ measured before ITO deposition. $R_{\mathrm{w\,ITO}}$ depends linearly on $R_{\mathrm{w/o\,ITO}}$. Therefore, Raman spectroscopy can be applied to finished solar cells to investigate the microstructure of the a-Si:H films.[16] Note that the absolute intensity of the Raman signal was higher because of the higher in-coupling of light due to the ITO coating.[48]

3. Discussion

The deposition parameters of the a-Si:H layers investigated in this paper are also used for the underdense i1 layer in the SHJ solar cell fabrication.[2,16,28,34,35] This layer is intended to improve the passivation of the c-Si surface by avoiding epitaxial growth using a fast (>1 nm s^{-1}) and disordered growth instead. For underdense a-Si:H a relatively high microstructure parameter is expected, as also found for our FTIR measurements shown in Figure 2.[2,28,34] The differences in R occurring due to the plasma power P_P variation can be explained by an increased ion bombardment of the a-Si:H film with increasing P_P. Increasing P_P increases the growth rate of the film up to a certain power.[49] In the power range we used, an increase of P_P increases the self-bias and thus the bombardment by H+ ions and therefore can lead to an ion-etching effect reducing the hydrogen content in the a-Si film and the microstructure parameter.[50,51] This change is clearly detected by both FTIR and Raman spectroscopy.

The microstructure parameter R_{IR} in Figure 2 determined by FTIR spectroscopy is higher for all samples than determined by Raman spectroscopy. However, R_{IR} measured by FTIR approaches R_R measured by Raman spectroscopy for thicker layers. In contrast to R_{IR}, R_R is constant for films with $d > 10$ nm. The differences between R_{IR} and R_R regarding the dependence on the a-Si:H thickness can partly occur due to the insensitivity of Raman spectroscopy (under our conditions) for Si—H bonds at the c-Si/a-Si:H interface. This assumption is consistent with the measurement in Figure 3 where Raman spectroscopy does not detect the hydrogen bonds on the c-Si surface, also in agreement

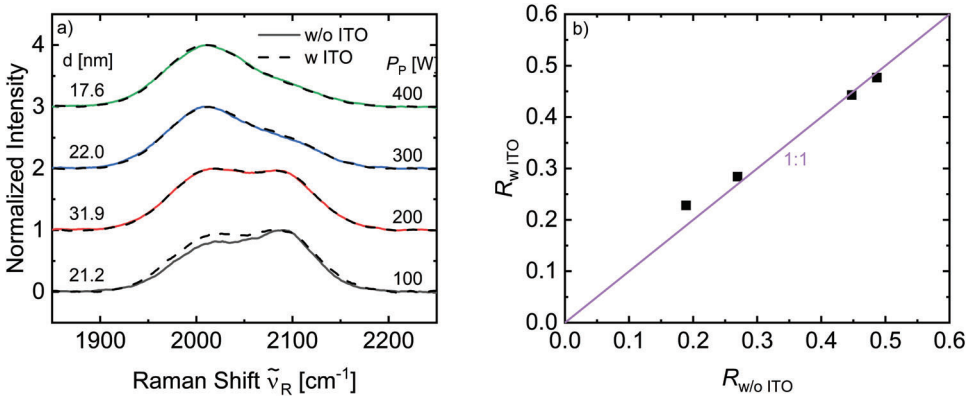

Figure 6. a) Raman intensity spectra of intrinsic a-Si:H layers versus the Raman shift $\tilde{\nu}_R$. All spectra are normalized by their maximum for better comparability. The plasma power was varied and is indicated on the right side of the graph. The layer thickness d is indicated on the left side of the graph. The solid lines show the spectra of the samples before, and the dashed lines show the spectra of the samples after ITO deposition. b) The microstructure parameter $R_{w\ ITO}$ measured after ITO deposition as a function of the microstructure parameter $R_{w/o\ ITO}$ measured before ITO deposition. The layer thickness is indicated above the FTIR measurements. The purple line indicates a 1:1 correlation.

with results by Spizzirri et al.[44] Therefore, the Raman spectra of our setup apparently provide information on the microstructure of the bulk a-Si:H and not on the Si—H bonds at the c-Si surface. This also holds for more dense a-Si:H as shown with a material also used in the i2-layer of SHJ solar cells.[34] Note that Si—H bonds at c-Si surfaces were detected also via Raman spectroscopy by Hines et al.,[52] but these measurements were made using polarized Raman spectroscopy under certain angles and the ratio of the Raman scattering intensity to the laser power was low compared to the ratio obtained by our measurements on a-Si:H films. FTIR spectroscopy, in contrast, is sensitive to the hydrogen bond configuration at the c-Si surface. These hydrogen bonds at the surface/interface contribute to the peak at 2100 cm^{-1} of the FTIR spectrum and therefore increase the microstructure parameter, especially for very thin layers.[13,24] However, the absorption at 2100 cm^{-1} within the spectrum of the Hf-dip in Figure 3 is not strong enough to fully explain the difference between FTIR and Raman microstructure factor. During the transport of the Hf-dipped wafer to the FTIR spectroscope, a loss of Si—H bond on the surface might occur, leading to a lower absorption signal. We used a simple model to calculate the possible influence of a fully H-covered c-Si surface on the FTIR absorption spectra. To calculate the thickness dependence of the FTIR microstructure parameter, the model combines a homogeneous a-Si:H layer with a single layer of hydrogen at the interface bonded to the c-Si surface, neglecting the existence of a nucleation layer. The calculation agrees with the measurement by fitting the ratio β of the absorption strength constants at the a-Si:H bulk and at the interface. Within this model, the absorption strength constant A within a-Si:H is up to 20 times higher than at the c-Si surface. The absorption strength at the surface can vary because of a different refractive index or dynamic charge.[14] However, an increase of a factor 20 is unlikely and not reported in the literature, indicating that H on the c-Si surface is not the only reason for the thickness dependence of the FTIR microstructure parameter. The interface hydrogen model can also be fitted to the measurements by using a higher amount of hydrogen n_{int} at the interface while using a constant absorption strength constant A (i.e., $\beta = 1$) for interface and a-Si:H bulk hydrogen. This would require more hydrogen than one monolayer. Besides the monolayer at the a-Si/c-Si interface, hydrogen can also be located at the a-Si:H surface on the front side of the film and at the cSi surface on the rear side of the substrate. However, these additional monolayers would result in a maximum total of 3 monolayers instead of 20 which are needed to explain the increase in R for thinner layers in Figure 4. Additional hydrogen contributing only to the 2100 cm^{-1} peak might be located at the nucleation region of the a-Si-H film.[24] The presence of a nucleation layer of ≈10 nm or less has also been modeled by Li et al.[53] The FTIR spectra indeed indicate an increased amount of Si—$H_{2/3}$ bonds. The characteristic bending modes of those bonds are located between 840 and 900 cm^{-1} and have the same intensity for all films shown in Figure 5 independent of the film thickness. The stretching modes of Si—$H_{2/3}$ bonds are assumed to contribute to the 2100 cm^{-1} peak since the bending modes could not be detected accompanied only by 2000 cm^{-1} stretching modes so far.[13,14,18] Cardona[14] found that for Si—$H_{2/3}$ stretching vibrations, all modes are in principle IR and Raman active, but for polarizability reasons, some modes actually show no Raman activity. In agreement with this, Zdetsis[54] found by ab initio calculations that embedded silicon fullerenes have three significant modes arising from Si—H stretching vibrations in infrared spectra, in contrast to only one dominant mode in Raman spectra. Fewer modes with significant Raman activity indicate that Si—$H_{2/3}$ bonds have less contribution to the 2100 cm^{-1} peak in comparison with the Si—H single bonds for Raman spectroscopy than for FTIR spectroscopy, which can be the second reason for the different thickness dependence of R in both methods. However, in general, a (less pronounced) signal from the Si—$H_{2/3}$ stretching modes should contribute to the Raman spectra as well, fitting to an increase in the Raman microstructure parameter for films >10 nm. In agreement with this, for our layers a decrease in the thickness normalized Raman intensities for layers with $d < 5$ nm was observed, and the shift of the 2100 cm^{-1} peak associated with the presence of Si—$H_{2/3}$ bonds could be observed in both Raman and FTIR spectra for our films with $d < 5$ nm (data not shown).[24]

Besides the eventual difference of Raman and FTIR spectra due to different Si—$H_{2/3}$ stretching mode activities, additional

effects can lower the signal of the Si—H bonds within the nucleation layer. The most obvious effect is that the laser intensity and therefore Raman scattering intensity decreases with higher penetration depths into the film. Therefore, the weight of the scattering intensity within the nucleation layer to the total scattering intensity decreases exponentially with increasing film thickness. Nevertheless, we found no significant influence of this effect for our rather thin films, since a linear increase of the Raman scattering intensity with the film thickness was observed (see Figure 2b). Further possible effects are for instance interference enhanced Raman scattering[55] effects or different dielectric properties of the nucleation region and so polarizability of the Si–H modes leading to lower Raman scattering intensities.[25] In addition, a high amount of hydrogen in the nucleation layer can extend the band gap of the aSi:H.[56] This is detrimental to the absorption of the 532 nm laser and therefore to the resonance Raman effect maybe occurring at the a-Si:H bulk material.[57]

Detected with FTIR, three components contribute to the microstructure parameter, namely the H at the c-Si surface, the H in the nucleation layer and the H in the bulk layer, while for the Raman microstructure parameter of our samples, the first component is missing and the H in the nucleation layer seems to be only weakly detected, leading to a constant R for layers with $d >$ 10 nm.

The R measured using Raman spectroscopy on textured wafers (hollow squares) in Figure 2d shows a similar trend as the R measured on polished wafers (filled squares), showing the ability to measure the microstructure direct on textured wafers.

Figure 6 shows that using Raman spectroscopy R of a-Si:H layers can be measured even covered by ITO and that at least in the range from $R = 0.2$ to $R = 0.5$ the microstructure is apparently not affected by our ITO sputtering process. The slight difference between the two spectra of the layer deposited at $P_p = 100$ W might occur by different measurement locations on the sample and is not necessarily caused by the ITO deposition. The fact that R for a-Si:H layers underneath ITO equals R for layers without ITO and that measurements on textured silicon substrates equals measurements on polished silicon substrates provides evidence that microstructure measurements on finished solar cells are possible and comparable to measurements on polished substrates. This enables a direct measurement of the microstructure of a-Si:H layers on finished solar cells and allows the investigation of the changes after further post-processing steps like annealing, light-soaking, or applying a hydrogen plasma.

4. Conclusion

The present paper demonstrates investigations of the microstructure parameter of a-Si:H thin films with a thickness of a few nanometers covered by ITO on polished c-Si substrates and on textured c-Si substrates using Raman spectroscopy in the backscattering regime. The method allows the investigation of R of a-Si:H layer stacks directly in a TCO-covered textured silicon solar cell on each side independently.

Our results show that for the comparison of the Raman and FTIR microstructure parameters three components are to consider, namely the H at the c-Si surface, the H in the nucleation layer, and the H in the a-Si:H bulk layer. Using our setup, Raman spectroscopy does not detect Si—H bonds at the c-Si surface. The H within the nucleation layer is only weakly detected, tentatively because of the weak detection of Si—$H_{2/3}$ bonds, which are present in greater amounts within the nucleation layer. Thus, using Raman spectroscopy the microstructure parameter of the a-Si:H is measured, without the contribution of H at the c-Si/a-Si:H interface leading to a constant R for layers with d > 10 nm. On the other hand, measuring R using FTIR spectroscopy on rather thin layers is strongly influenced by the hydrogen at the c-Si/a-Si:H interface. Hence, for a-Si:H layers with similar microstructure but different thicknesses, FTIR spectroscopy will give different microstructure parameters as the contribution of H at the c-Si wafer is measured as well. Using the difference between the R measured using FTIR- and Raman spectroscopy as a tool provides deeper insight into the Si—H bonding structure and therefore into the surface passivation of SHJ solar cells.

5. Experimental Section

For a-Si:H sample preparation, an AK1000 PECVD system from Meyer Burger with a plasma excitation frequency of 13.56 MHz, an electrode area of (500 × 500) $mm^{2,}$ and an electrode gap of ≈17 mm was used. A substrate temperature $T = 200$ °C, a pressure $p = 2.7$ mbar, and a silane flow of $Q_{SiH4} = 145$ sccm without hydrogen dilution were applied to deposit layers with thicknesses from 2 to 61 nm by varying the deposition time and using plasma powers P_p of 100, 200, 300 and 400 W on one side of the substrates. These deposition parameters were also used in the solar cells to deposit a ≈2–3 nm thick layer of "underdense" a-Si:H on the c-Si surface to avoid epitaxial growth (i1-layer).[16,34] Therefore, the layers investigated in this work were supposed to grow highly disordered and had relatively high microstructure parameters compared to dense high-quality a-Si:H films with a low defect density.[17,35] Additionally, for comparison, a dense layer was prepared using similar deposition conditions as for the i2 layer in Duan et al.[34] with a 1/6.2 silane to hydrogen ratio and a plasma power P_p of 50 W. The layers were prepared on polished p-type high resistivity c-Si (100) float-zone wafers (525 µm, 20 Ωcm) etched in a 1% diluted hydrofluoric (HF) acid solution. In addition, some layers were also prepared on textured n-type Czochralski wafers from Longi (135 µm, 1 Ωcm). The n-type c-Si wafers were textured using the SHJ solar cell baseline process as described by Duan et al.[34] For the investigation of the microstructure underneath ITO, 4 layers were chosen on HF-etched polished c-Si with similar thicknesses (17– 31 nm), each deposited at different plasma powers. After measuring the samples by FTIR and Raman spectroscopy, ITO (70 nm) as used for SHJ solar cells was deposited on these samples to compare the microstructure before and after ITO deposition. The ITO layers were sputtered with a direct current mode from a 3% Sn-doped In_2O_3 target. The working pressure was set to 0.3 Pa with a partial oxygen pressure of 0.016 Pa using a fixed total argon and oxygen flow rate of 95 sccm. Further details could be found in Duan et al.[34]

The thicknesses of the layers on the polished samples were determined by spectroscopic ellipsometry using a T-Solar/M2000 from J.A. Woollam. A Renishaw inVia Raman spectrometer with a 532 nm laser was used in the back-scattering configuration without a polarization analyzer to investigate the Raman scattering of the samples. Photothermal deflection spectroscopy (PDS) measurement (on samples of ≈100 nm for a higher signal) showed that the (dense i2-layer) a-Si:H had an absorption coefficient of ≈0.01 nm^{-1} for green light (532 nm), which meant that the laser intensity was reduced to the fraction of 1/e in a penetration depths of 100 nm in agreement with Beyer et al.[58] The penetration depth of this underdense material could vary a little from that of the dense i2 layer but should be within the same scale. The laser intensity was set to 2.5 mW using a Gaussian-shaped circular beam with a diameter of 2–3 µm. Differences in the microstructure of a-Si:H were unlikely caused by the Raman laser heating since results were obtained independent of the intensity of the laser, indicating that the temperature was below the hydrogen effusion or silicon

crystallization thresholds. The FTIR spectra of the samples on polished c-Si substrates (without ITO) were measured using a Nicolet 5700 system from Thermo Electron Corporation in the range from 400 to 4000 cm^{-1}.

Acknowledgements

The authors gratefully acknowledge the SHJ baseline team of the IEK-5 for their help with the sample preparation.

Open access funding enabled and organized by Projekt DEAL.

Conflict of Interest

The authors declare no conflict of interest.

Data Availability Statement

The data that support the findings of this study are available from the corresponding author upon reasonable request.

Keywords

amorphous silicon, FTIR (Fourier transform infrared), passivation, Raman, silicon heterojunction

Received: June 30, 2023
Revised: August 29, 2023
Published online: October 16, 2023

[1] H. Lin, M. Yang, X. Ru, G. Wang, S. Yin, F. Peng, C. Hong, M. Qu, J. Lu, L. Fang, C. Han, P. Procel, O. Isabella, P. Gao, Z. Li, X. Xu, *Nat. Energy* **2023**, *8*, 789.
[2] H. Sai, P.o-W. Chen, H.-J. Hsu, T. Matsui, S. Nunomura, K. Matsubara, *J. Appl. Phys.* **2018**, *124*, 103102.
[3] R. Ishihara, J. Zhang, M. Trifunovic, M. Van Der Zwan, H. Takagishi, R. Kawajiri, T. Shimoda, C. I. M. Beenakker, *ECS Trans.* **2013**, *50*, 49.
[4] S. Han, X. Dai, P. Loy, J. Lovaasen, J. Huether, J. M. Hoey, A. Wagner, J. Sandstrom, D. Bunzow, O. F. Swenson, I. S. Akhatov, D. L. Schulz, *J. Non-Cryst. Solids* **2008**, *354*, 2623.
[5] B. Wu, C. Chen, D. L. Danilov, R.-A. Eichel, P. H. L. Notten, *Batteries* **2023**, *9*, 186.
[6] R. V. K. Chavali, S. De Wolf, M. A. Alam, *Prog. Photovoltaics* **2018**, *26*, 241.
[7] M. Tanaka, M. Taguchi, T. Matsuyama, T. Sawada, S. Tsuda, S. Nakano, H. Hanafusa, Y. Kuwano, *Jpn. J. Appl. Phys.* **1992**, *31*, 3518.
[8] S. De Wolf, A. Descoeudres, Z. C. Holman, C. Ballif, *Green* **2012**, *2*, 7.
[9] A. Descoeudres, L. Barraud, S. D. Wolf, B. Strahm, D. Lachenal, C. Guérin, Z. C. Holman, F. Zicarelli, B. Demaurex, J. Seif, J. Holovsky, C. Ballif, *Appl. Phys. Lett.* **2011**, *99*, 123506.
[10] M. Z. Burrows, U. K. Das, R. L. Opila, S. De Wolf, R. W. Birkmire, *J. Vac. Sci. Technol., A* **2008**, *26*, 683.
[11] M. Taguchi, A. Yano, S. Tohoda, K. Matsuyama, Y. Nakamura, T. Nishiwaki, K. Fujita, E. Maruyama, *IEEE J. Photovoltaics* **2014**, *4*, 96.
[12] H. Sai, T. Oku, Y. Sato, M. Tanabe, T. Matsui, K. Matsubara, *Prog. Photovoltaics* **2019**, *27*, 1061.
[13] H. Wagner, W. Beyer, *Solid State Commun.* **1983**, *48*, 585.
[14] M. Cardona, *Phys. Status Solidi B* **1983**, *118*, 463.
[15] L. Zhao, H. Diao, X. Zeng, C. Zhou, H. Li, W. Wang, *Phys. B* **2010**, *405*, 61.
[16] B. Fischer, W. Beyer, A. Lambertz, M. Nuys, W. Duan, K. Ding, U. Rau, *Sol. RRL* **2023**, *7*, 2300103.
[17] W. Beyer, M. S. A. Ghazala, *MRS Proc.* **1998**, *507*, 601.
[18] M. H. Brodsky, M. Cardona, J. J. Cuomo, *Phys. Rev. B* **1977**, *16*, 3556.
[19] H. Shanks, C. J. Fang, L. Ley, M. Cardona, F. J. Demond, S. Kalbitzer, *Phys. Status Solidi B* **1980**, *100*, 43.
[20] A. H. M. Smets, W. M. M. Kessels, M. C. M. Van De Sanden, *Appl. Phys. Lett.* **2003**, *82*, 1547.
[21] A. H. M. Smets, M. C. M. Van De Sanden, *Phys. Rev. B* **2007**, *76*, 073202.
[22] D. Jousse, E. Bustarret, F. Boulitrop, *Solid State Commun.* **1985**, *55*, 435.
[23] A. H. Mahan, P. Raboisson, R. Tsu, *Appl. Phys. Lett.* **1987**, *50*, 335.
[24] H. Fujiwara, Y. Toyoshima, M. Kondo, A. Matsuda, *Phys. Rev. B* **1999**, *60*, 13598.
[25] A. Canillas, E. Bertran, J. L. Andújar, B. Drévillon, *J. Appl. Phys.* **1990**, *68*, 2752.
[26] Y. Zhao, P. Procel, A. Smets, L. Mazzarella, C. Han, G. Yang, L. Cao, Z. Yao, A. Weeber, M. Zeman, O. Isabella, *Prog. Photovoltaics* **2022**, 1.
[27] C. Maurer, S. Haas, W. Beyer, F. C. Maier, U. Zastrow, M. Hülsbeck, U. Breuer, U. Rau, *Thin Solid Films* **2018**, *653*, 223.
[28] W. Liu, L. Zhang, R. Chen, F. Meng, W. Guo, J. Bao, Z. Liu, *J. Appl. Phys.* **2016**, *120*, 175301.
[29] J. Melskens, A. H. M. Smets, M. Schouten, S. W. H. Eijt, H. Schut, M. Zeman, presented at *IEEE 38th Photovoltaic Specialists Conference (PVSC) PART 2*, Austin, TX, USA, June **2012**.
[30] W. Beyer, in *Semiconductors and Semimetals*, vol. *61* (Ed.: N. H. Nickel), Elsevier, Amsterdam, Netherlands, **1999**, pp. 165.
[31] K. Pangal, J. C. Sturm, S. Wagner, T. H. Büyüklimanli, *J. Appl. Phys.* **1999**, *85*, 1900.
[32] R. Saive, M. Boccard, T. Saenz, S. Yalamanchili, C. R. Bukowsky, P. Jahelka, Z. J. Yu, J. Shi, Z. Holman, H. A. Atwater, *Sustainable Energy Fuels* **2017**, *1*, 593.
[33] M. A. Green, M. J. Keevers, *Prog. Photovoltaics* **1995**, *3*, 189.
[34] W. Duan, A. Lambertz, K. Bittkau, D. Qiu, K. Qiu, U. Rau, K. Ding, *Prog. Photovoltaics* **2022**, *30*, 384.
[35] X. Ru, M. Qu, J. Wang, T. Ruan, M. Yang, F. Peng, W. Long, K. Zheng, H. Yan, X. Xu, *Sol. Energy Mater. Sol. Cells* **2020**, *215*, 110643.
[36] V. A. Volodin, D. I. Koshelev, *J. Raman Spectrosc.* **2013**, *44*, 1760.
[37] B. Macco, J. Melskens, N. J. Podraza, K. Arts, C. Pugh, O. Thomas, W. M. M. Kessels, *J. Appl. Phys.* **2017**, *122*, 035302.
[38] Z. Wu, L. Zhang, R. Chen, W. Liu, Z. Li, F. Meng, Z. Liu, *Appl. Surf. Sci.* **2019**, *475*, 504.
[39] A. Soman, U. Nsofor, U. Das, T. Gu, S. Hegedus, presented at *IEEE 46th Photovoltaic Specialists Conference (PVSC)*, Chicago, IL, USA, June **2019**.
[40] J. Holovský, S. De Wolf, P. Jiříček, C. Ballif, *Rev. Sci. Instrum.* **2015**, *86*, 073108.
[41] X. H. Sun, S. D. Wang, N. B. Wong, D. D. D. Ma, S. T. Lee, B. K. Teo, *Inorg. Chem.* **2003**, *42*, 2398.
[42] S. N. Granata, T. Bearda, F. Dross, I. Gordon, J. Poortmans, R. Mertens, *Energy Procedia* **2012**, *27*, 412.
[43] H. Sano, S. Ushioda, *Phys. Rev. B* **1996**, *53*, 1958.
[44] P. G. Spizzirri, 'Nano-Raman spectroscopy of silicon surfaces', p. 5.
[45] A. A. Langford, M. L. Fleet, B. P. Nelson, W. A. Lanford, N. Maley, *Phys. Rev. B* **1992**, *45*, 13367.
[46] L. Zhang, W. Guo, W. Liu, J. Bao, J. Liu, J. Shi, F. Meng, Z. Liu, *J. Phys. D: Appl. Phys.* **2016**, *49*, 165305.
[47] R. A. Street, *Hydrogenated amorphous silicon*, Cambridge University Press, New York **1991**.
[48] J. Pla, M. Tamasi, R. Rizzoli, M. Losurdo, E. Centurioni, C. Summonte, F. Rubinelli, *Thin Solid Films* **2003**, *425*, 185.
[49] Y. Y. Ong, B. T. Chen, F. E. H. Tay, C. Iliescu, *J. Phys.: Conf. Ser.* **2006**, *34*, 812.

[50] Y. Kuo, *J. Electrochem. Soc.* **1990**, *137*, 1235.
[51] N. Maître, T.h. Girardeau, S. Camelio, A. Barranco, D. Vouagner, E. Breelle, *Diamond Relat. Mater.* **2003**, *12*, 988.
[52] M. A. Hines, Y. J. Chabal, T. D. Harris, A. L. Harris, *J. Chem. Phys.* **1994**, *101*, 8055.
[53] D. Li, G. L. Liu, Y. Yang, J. H. Wu, Z. R. Huang, *J. Nanomater.* **2013**, *2013*, 383867.
[54] A. D. Zdetsis, *Phys. Rev. B* **2009**, *79*, 195437.
[55] G. A. N. Connell, R. J. Nemanich, C. C. Tsai, *Appl. Phys. Lett.* **1980**, *36*, 31.
[56] (Eds.: H. Fujiwara, R. W. Collins), *Spectroscopic Ellipsometry for Photovoltaics: 1: Fundamental Principles and Solar Cell Characterization*, 1st edn., Springer, Cham, Switzerland **2018**.
[57] J. R. Ferraro, K. Nakamoto, C. W. Brown, in *Introductory Raman Spectroscopy (Second Edition)*, (Eds.: J. R. Ferraro, K. Nakamoto, C. W. Brown), Academic Press, San Diego **2003**, pp. 1–94.
[58] W. Beyer, G. Andrä, J. Bergmann, U. Breuer, F. Finger, A. Gawlik, S. Haas, A. Lambertz, F. C. Maier, N. H. Nickel, U. Zastrow, *J. Appl. Phys.* **2018**, *124*, 153103.